AD-A137 199 A CALCULATION OF DESCENT SEGMENT OF INTERNAL BALLISTICS 1/1
IN SOLID ROCKET MOTORS(U) FOREIGN TECHNOLOGY DIV
WRIGHT-PATTERSON AFB OH F DINGYOU 05 JAN 84
UNCLASSIFIED FTD-ID(RS)T-1819-83 F/G 21/8.2 NL

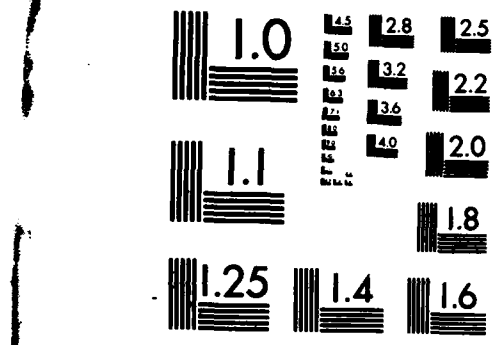

(2)

FTD-ID(RS)T-1819-83

FOREIGN TECHNOLOGY DIVISION

A CALCULATION OF DESCENT SEGMENT OF INTERNAL BALLISTICS IN SOLID ROCKET MOTORS

by

F. Dingyou

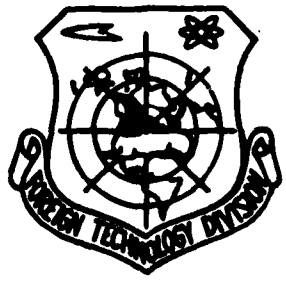

EDITED TRANSLATION

FTD-ID(RS)T-1819-83 5 January 1984

MICROFICHE NR: FTD-84-C-00007

A CALCULATION OF DESCENT SEGMENT OF INTERNAL BALLISTICS IN SOLID ROCKET MOTORS

By: F. Dingyou

English pages: 13

Source: Yuhang Xuebao, Vol. 1, Nr. 1, 1983, pp. 29-36

Country of origin: China
Translated by: LEO KANNER ASSOCIATES
F33657-81-D-0264
Requester: FTD/SDBS

PREPARED BY:

TRANSLATION DIVISION
FOREIGN TECHNOLOGY DIVISION
WP-AFB, OHIO.

GRAPHICS DISCLAIMER

All figures, graphics, tables, equations, etc. merged into this translation were extracted from the best quality copy available.

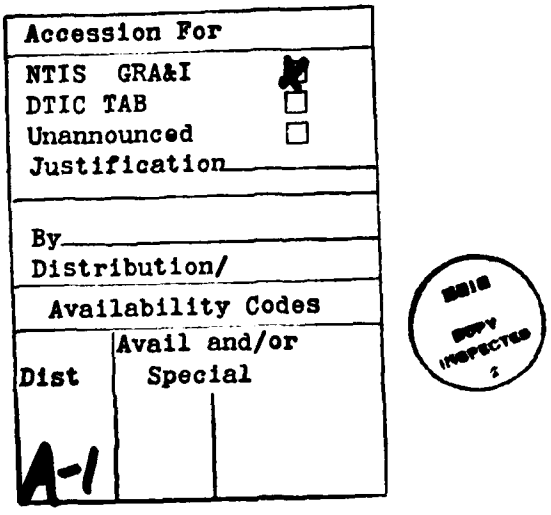

A CALCULATION OF DESCENT SEGMENT OF INTERNAL BALLISTICS IN SOLID ROCKET MOTORS

Fang Dingyou

Abstract

The precise prediction of the after-working impulse of solid rocket motors is very important for the prediction of missile and motor performance. This paper uses the characteristic method to consider the changes of gaseous parameters along the combustion chamber length and to calculate the descent segment of internal ballistics in solid rocket motors. The gaseous parameters in the descent segment along the combustion chamber length which change with time are given and the calculation results of the characteristic method and isentropic model are compared.

I. Preface

The precise prediction of the after-working impulses of solid rocket motors is very important for the prediction of missile and motor performance. In the past, calculations of the descent segments of internal ballistics in solid rocket motors viewed the gas in the combustion chamber when the charge is burned up as the isentropic gas of uniform stagnation and assumed that it changes according to the isentropic process (abbreviated as the isentropic model). However, in reality, the gas parameters when the charge is burned up are: the changes of the velocity, pressure, temperature and density along the length of the combustion chamber; because of the influence of the added flow when the charge burns, the entropy of the gas on each section of the combustion chamber in the descent segment are not equal. Therefore, based on the calculation of the isentropic model, how large are the errors which

can finally be carried along? This paper uses the characteristic method to consider the changes of the gas parameters along the length of the combustion chamber to calculate the descent segment of the internal ballistics and makes comparisons with the calculations of the isentropic model.

II. Control Equations

Hypotheses:

1. We only consider that the unsteady flow of the gas in the combustion chamber and the nozzle flow is quasi-stationary. Because the nozzle volume is much smaller than the volume of the combustion chamber, this hypothesis is appropriate; on the other hand, in order to reduce the computer time, we consider that the unsteady flow of the nozzle's changing section greatly reduces the length of the computation steps and causes the computer time to increase several times or several tens of times.

2. The combustion gas is completely gas and the flow is one-dimensional.

3. At the same time the charge on each section of the combustion chamber is burning up, this hypothesis makes the computation of the descent segment convenient. If we have already completely computed the internal ballistics of the motor's operating section and we know the distribution of the gas parameters along the length of the combustion chamber when the charge is burned up, we can then cancel this hypothesis.

4. The combustion chamber is a uniform gas passage.

5. We do not consider that the combustion of the adiabatic layer is equal in the descent segment.

Under these hypotheses, the control equations are:

Continuity equation

$$\frac{\partial \rho}{\partial t} + u\frac{\partial \rho}{\partial x} + \rho\frac{\partial u}{\partial x} = 0$$

Momentum equation

$$\rho\frac{\partial u}{\partial t} + \rho u\frac{\partial u}{\partial x} + \frac{\partial p}{\partial x} = 0$$

Energy equation

$$\frac{\partial p}{\partial t} + u\frac{\partial p}{\partial x} - a^2\left(\frac{\partial \rho}{\partial t} + u\frac{\partial \rho}{\partial x}\right) = 0$$

Gas state equation

$$p = \rho RT$$

Velocity of sound

$$a = \sqrt{\gamma\frac{p}{\rho}}$$

In the formulas, u, T, ρ, p, a and y are the velocity of flow, temperature, density, pressure, velocity of sound and specific heat ratio of the gas. This is a set of hyperbolic partial differential equations which can be solved by the characteristic method. The characteristic equations and compatibility equations are:

Characteristic equations

$$\left(\frac{dt}{dx}\right)_0 = \lambda_0 = \frac{1}{u} \quad (\text{(1)})$$

$$\left(\frac{dt}{dt}\right)_\pm = \lambda_\pm = \frac{1}{u \pm a} \quad (\text{(2)})$$

Key: (1) Trajectory; (2) Mach line.

Compatibility equations

$$dp_0 - a^2 d\rho_0 = 0 \text{ (沿轨线)} \quad (1)$$
$$dp_0 \pm \rho a du_0 = 0 \text{ (沿马赫线)} \quad (2)$$

Key: (1) Along the trajectory; (2) Along the Mach line.

In the formulas, corner note "0" or "t" indicate along the trajectory or along the right and left lines.

This paper uses the contragradient method limited difference algorithm to carry out computations and the computations of the initial values are determined by the computation of the added flow the instant the charge burns out.

III. Computation Examples

Fig. 1 shows the computed motor. Fig. 2 shows the calculation of the distribution of the beginning instantaneous entropic increase along the length of the combustion chamber. This is created by the added flow.

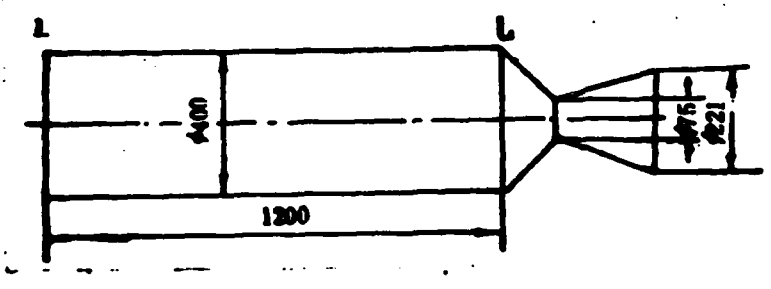

Fig. 1 Computed motor.

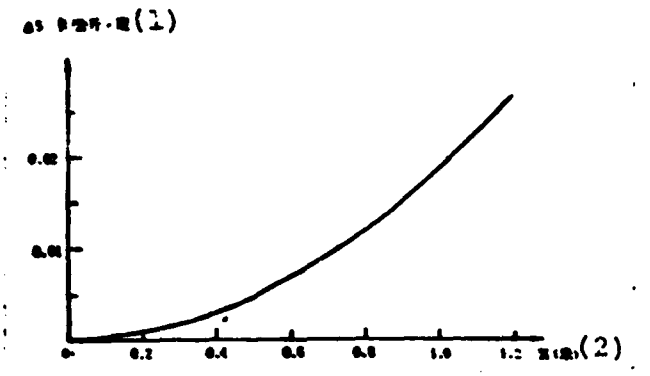

Fig. 2 Distribution of entropic increase along the length of the combustion chamber when t=0.

Key: (1) Calories/kg·degrees; (2) Meters.

Figs. 3a and 3b show that the velocity of flow of gas changes with time. Fig. 3a shows the situation of the descent segment within the beginning 3 milliseconds and Fig. 3b shows the situation within 4 milliseconds after 60 milliseconds in the descent segment. We can see from the figures that aside from the velocity of flow of the front end being zero and the rear end velocity of flow monotonously reduced, the velocities of flow on the other sections which change with time all assume vibration characteristics. Because the times the disturbance waves in the nozzle entrance area are propagated to each section are different, the oscillation characteristics of the velocity of flow on each section are also different. We can see from Fig. 3a that when the disturbance is propagated to a certain section, the velocity of flow of that certain section has maximum value and after the disturbance wave has passed, its velocity of flow then decreases. By comparing Figs. 3a and 3b, we can see that the oscillation period of the velocity of flow enlarges with the passage of time and the amplitude of the oscillation decreases with the passage of time. We can see from Fig. 3a that the oscillation period is 1.8 milliseconds and we can see from Fig. 3b that the oscillation period is 2.15 milliseconds.

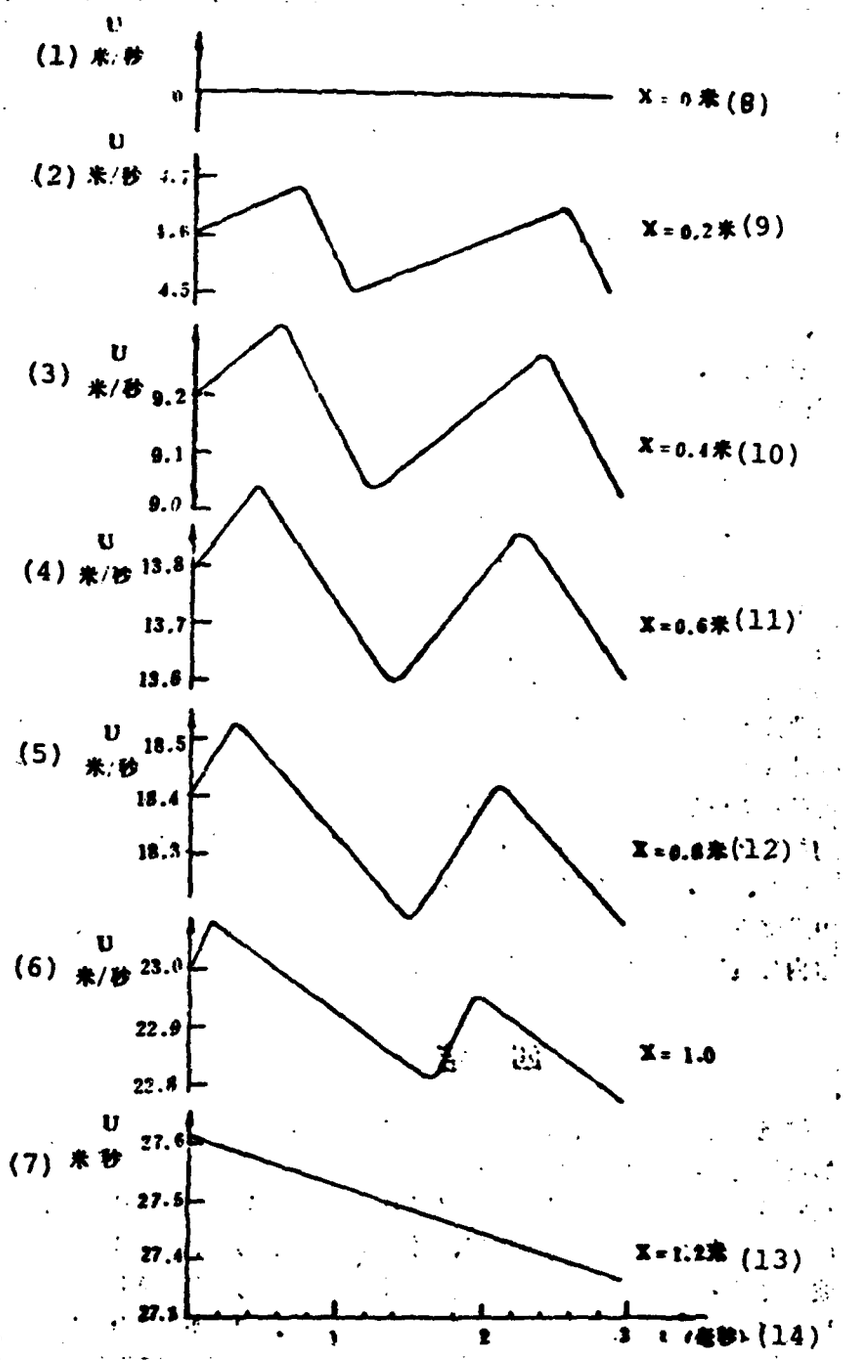

Fig. 3a Velocity of flow on each section of the combustion chamber changes with time.

Key: (1)-(7) Meters/second; (8)-(13) Meters; (14) Milliseconds.

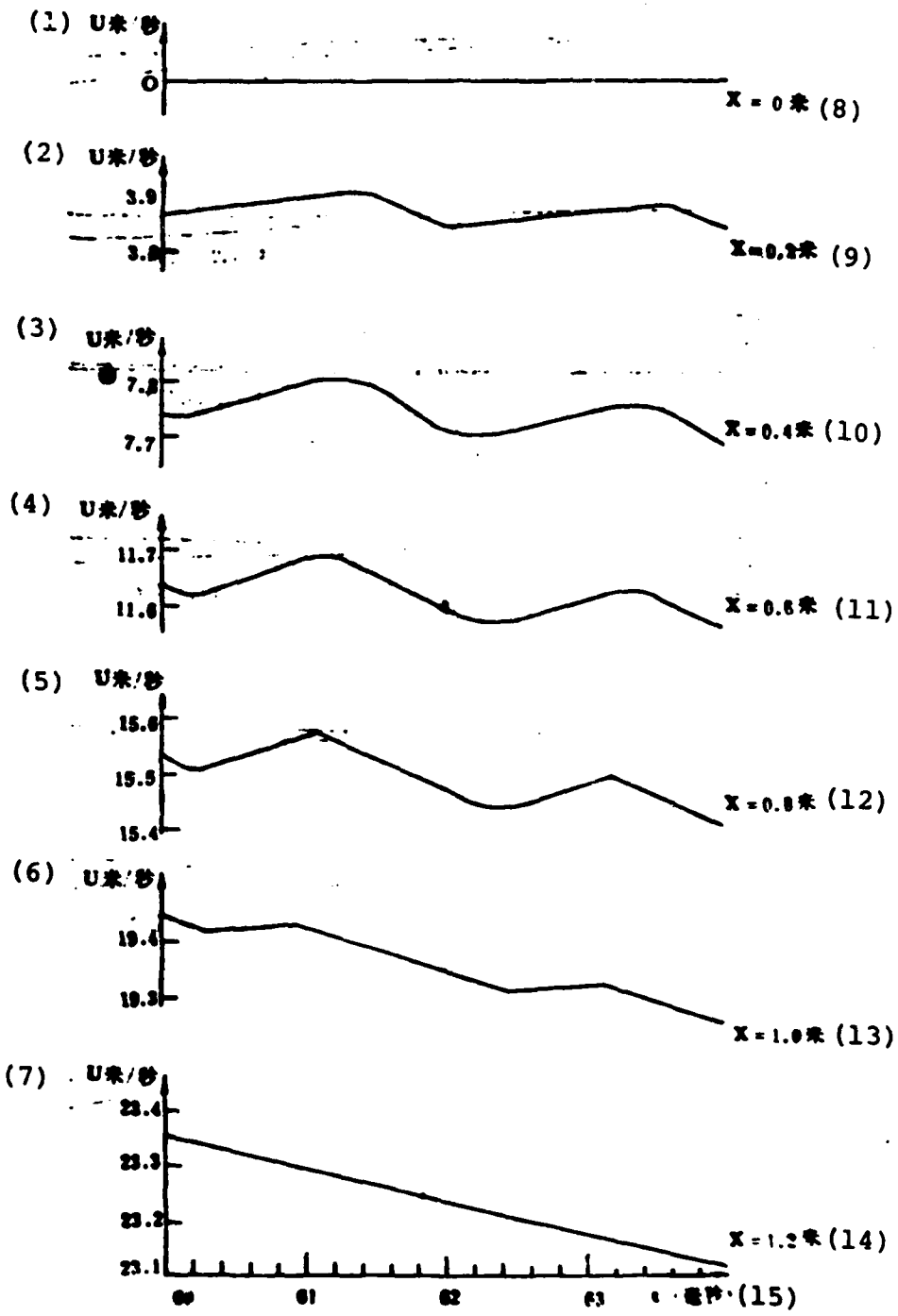

Fig. 3b Velocity of flow on each section of the combustion chamber changes with time.

Key: (1)-(7) Meters/second; (8)-(14) Meters; (15) Millimeters.

Fig. 4 shows that the distribution of the pressure and total pressure along the axis of the combustion chamber change with time. Fig. 5 shows that the average pressure of the combustion chamber changes with time. We can see from Figs. 4 and 6 that the general tendency of these parameters which change with time is to become smaller and smaller. However, they are distributed along the axis and sometimes the front end is higher than the rear end and sometimes the rear end is higher than the front end and assumes oscillation characteristics. As shown in Fig. 5, the ratio of rear end pressure p_L total pressure p_{SL} and temperature T_L, and front end pressure p_1, total pressure p_1 and temperature T_1 changes with time, its oscillation period and velocity of flow are the same and it is the time the disturbance wave is propaged back and forth once in the combustion chamber. The oscillation period within the initial several milliseconds of the descent segment is 1.8 milliseconds.

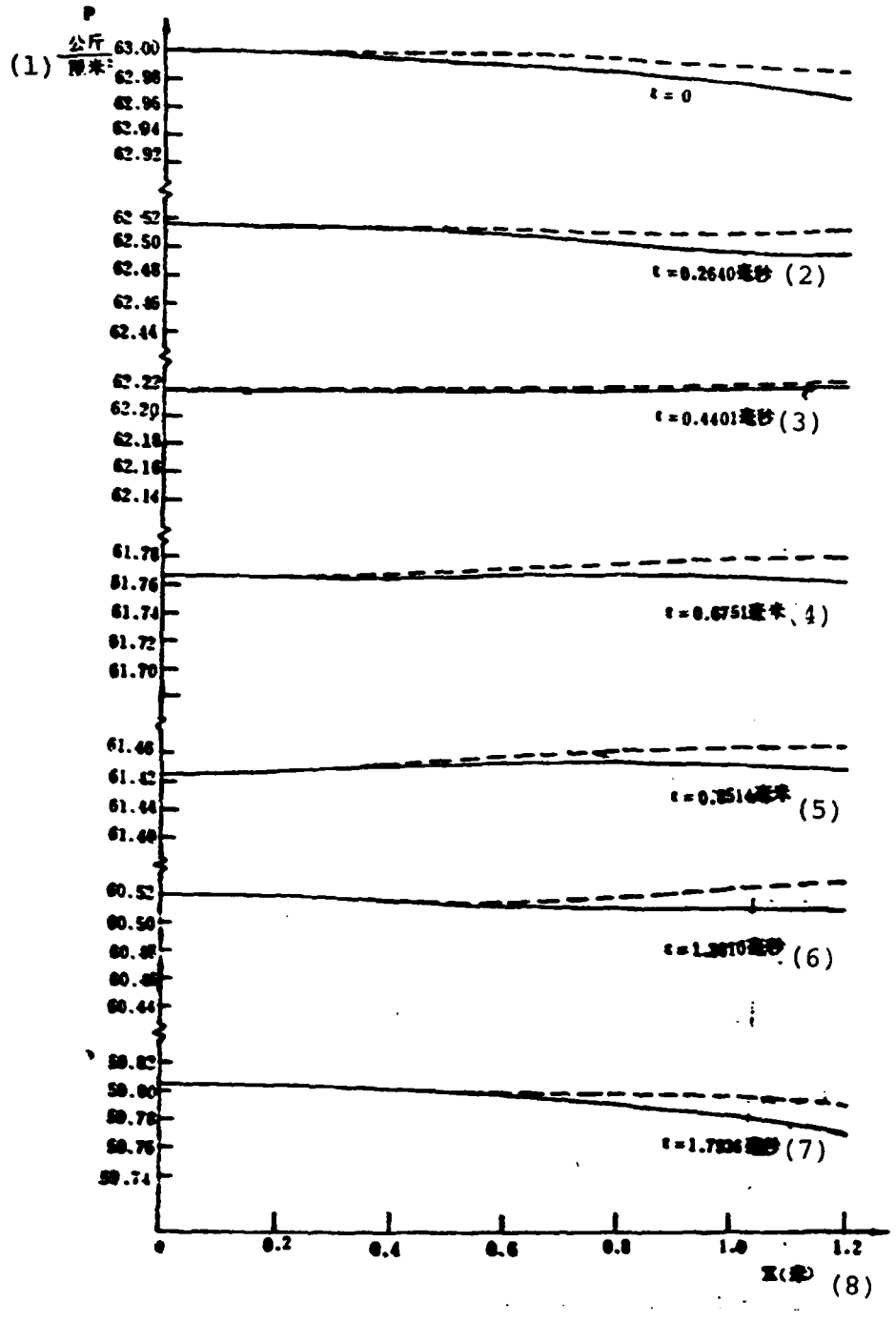

Fig. 4 The combustion chamber pressure distributed along the axis changes with time.——— static pressure,..... total pressure.

Key: (1) Kg/cm^2; (2)-(7) Millimeters; (8) Meters.

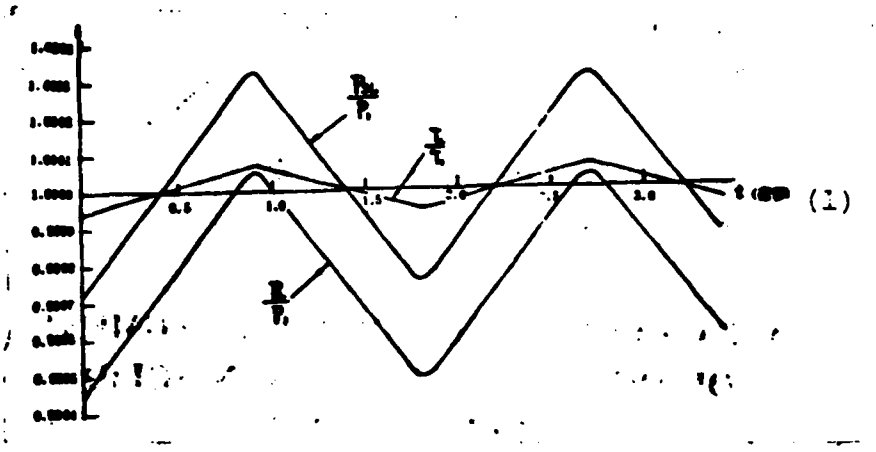

Fig. 5 $\frac{P_L}{P_1}$, $\frac{P_{SL}}{P_1}$ and $\frac{T_L}{T_1}$ change with time.

Key: (1) Milliseconds.

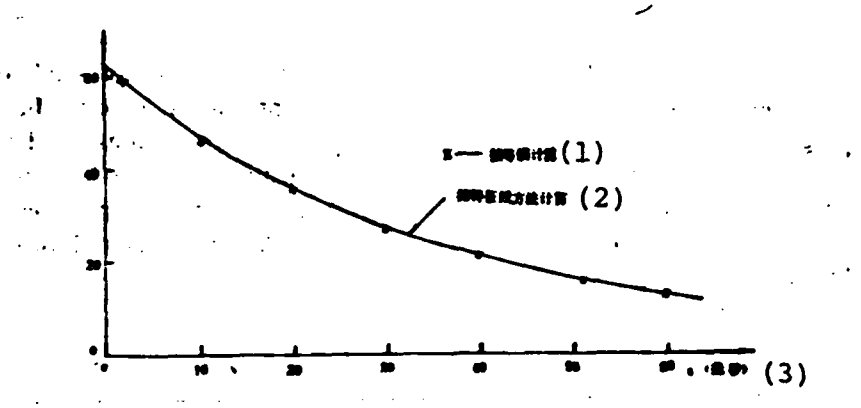

Fig. 6 The combustion chamber pressure changes with time.

Key: (1) Calculated according to the idrnytopy; (2) Calculated according to the characteristic method; (3) Milliseconds.

Fig. 6 shows the average combustion chamber pressure calculated according to the characteristic method and the combustion chamber pressure which is calculated according to the isentropic model and changes with time. The initial value of the

descent segment calculated according to the characteristic method is calculated by the equilibrium pressure formula. We can see from the figure that the combustion chamber pressure calculated according to the isentropic model is slightly lower than the value calculated by the characteristic method. Fig. 7 shows the motor's vacuum thrust taking into consideration the unsteady flow in the combustion chamber and the motor's vacuum thrust which is calculated according to the isentropic model and changes with time. Because the influence of the unsteady process in the combustion chamber on the thrust is very small, the thrust curve is similar to the combustion chamber's pressure curve and the thrust calculated according to the isentropy is slightly lower than the value calculated by the characteristic method. Calculations show that the differences of the above curves are mainly due to the differences of the initial pressure (the pressure of the initial point of the descent segment) value. The pressure value calculated according to the equilibrium pressure formula is lower than the average combustion chamber pressure obtained by calculating the added flow in the uniform passage. If the initial combustion chamber pressure calculated by the isentropic model is equal to the average value of the initial pressure calculated by the characteristic method, then the calculation results of the two methods are very close. Therefore, if we do not study the distribution of the gas parameters along the combustion chamber axis but only study the design of the after-working impulse of the motor or combustion chamber pressure in the descent segment and the motor's thrust which changes with time, we can calculate according to the isentropic model. However, the initial pressure must use the average combustion chamber pressure obtained from the added flow in the uniform passage.

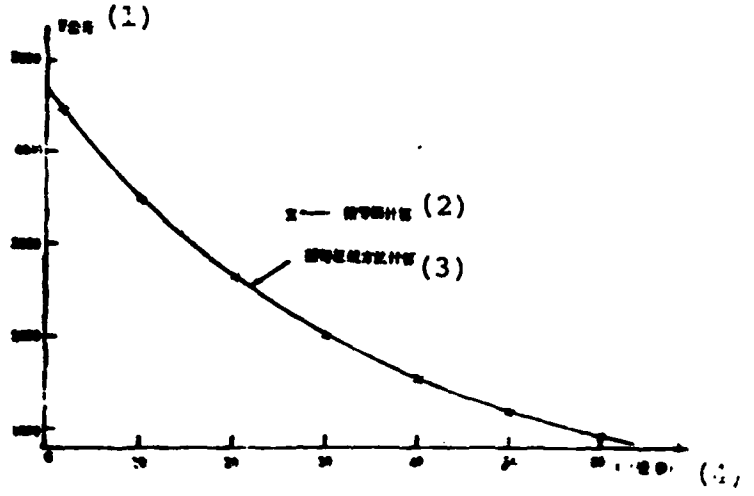

Fig. 7 The thrust changes with time.

Key: (1) Kg; (2) Calculated according to the isentropy; (3) Calculated according to the characteristic method; (4) Milliseconds.

IV. Conclusions

1. Because the combustion chamber has the propagation of disturbance waves originating from the area of the nozzle entrance, in the combustion chamber, aside from the front end and rear end, the gas velocity of flow on each section which changes with time assumes oscillation characteristics.

2. The ratio of the combustion chamber's rear end pressure, total pressure and temperature, and the front end pressure, total pressure and temperature which changes with time also assumes oscillation characteristics. Its oscillation period is equal to the time required for the disturbance waves to be propagated from the rear end to the front end and then from the front end to the rear end. Because the propagation speed of the disturbance waves in the descent process gradually decreased, the oscillation period enlarged with the passage of time.

3. The ranges of the pressure and temperature changes along the length of the combustion chamber were extremely small. Moreover, the gas velocity of flow in the combustion chamber was very low and its influence on the pressure and temperature was very small. Therefore, the pressure and temperature on each section of the combustion chamber which change with time do not resemble the oscillation of the velocity of flow but have monotonous descent. However, sometimes the descent is relatively fast and sometimes it is relatively slow.

4. If we do not study the gas flow parameters in the combustion chamber which are distributed along the axis and change with time but only consider the calculation of the motor's after-working impulse, we can use the isentropic model. However, the initial pressure must use the average pressure obtained by calculating the added flow when the charge burns up.

5. Because the pressure difference of the combustion chamber's front end and rear end is not large, the gas velocity of flow of the combustion chamber's rear end is not large, the influence of the unsteady flow in the combustion chamber on the motor's thrust is not large and when calculating the after-working impulse of the motor, we can not calculate the unsteady flow in the combustion chamber.

References

[1] Maurice J. Zucrow, J.D. Hoffman, "Gas Dynamics," Volume II, 1976.

DISTRIBUTION LIST

DISTRIBUTION DIRECT TO RECIPIENT

ORGANIZATION	MICROFICHE
A205 DMAHTC	1
A210 DMAAC	1
B344 DIA/RTS-2C	9
C043 USAMIIA	1
C500 TRADOC	1
C509 BALLISTIC RES LAB	1
C510 R&T LABS/AVRADCOM	1
C513 ARRADCOM	1
C535 AVRADCOM/TSARCOM	1
C539 TRASANA	1
C591 FSTC	4
C619 MIA REDSTONE	1
D008 NISC	1
E053 HQ USAF/INET	1
E403 AFSC/INA	1
E404 AEDC/DOF	1
E408 AFWL	1
E410 AD/IND	1
E429 SD/IND	1
P005 DOE/ISA/DDI	1
P050 CIA/OCR/ADD/SD	2
AFIT/LDE	1
FTD	
CCN	1
NIA/PHS	1
NIIS	2
LLNL/Code L-389	1
NASA/NST-44	1
NSA/1213/TDL	2